International Journal of Nanoelectronics and Materials
Volume 15 (Special Issue) March 2022 [219-231]

Fabrication of Superhydrophobic Polyacrylonitrile (PAN) Nanofibres Membranes for Membrane Distillation Technology

M. W. Azmil Arif[1], A. H. Nurfaizey[1,2]*, M. Z. Akop[1,2], M. R. Mansor[1,2], J. Jaafar[3] and M. H. D. Othman[3]

[1]Fakulti Kejuruteraan Mekanikal, Universiti Teknikal Malaysia Melaka,
Hang Tuah Jaya, 76100 Durian Tunggal, Melaka, Malaysia
[2]Centre for Advanced Research on Energy, Universiti Teknikal Malaysia Melaka,
Hang Tuah Jaya, 76100 Durian Tunggal, Melaka, Malaysia
[3]Advanced Membrane Technology Research Centre (AMTEC), Universiti Teknologi Malaysia,
81310 Skudai, Johor, Malaysia

ABSTRACT

Membrane distillation (MD) is a promising water desalination technology that is capable of treating high salinity water. However, the problematic fouling issues and membrane wetting are the primary impediments to the large-scale application of this technology. To overcome the mentioned problems, the distilling membrane should be made from anti-wetting materials and possess a highly porous structure. In this study, a superhydrophobic nanofibrous membrane was fabricated through surface coating of electrospun polyacrylonitrile (PAN) nanofibres membranes using silica nanoparticles and fluorinated alkyl silane surface treatment. The coated PAN nanofibre membranes were characterised using scanning electron microscope (SEM), water contact angle (WCA) method, Fourier transform infrared (FTIR) and differential scanning calorimetry (DSC). It was observed that the amount and size of silica nanoparticle were related to hydrolysis time, which was crucial in determining the membrane pore size and formation of superhydrophobic surface. The presence of silica nanoparticles and fluorine content significantly improved the hydrophobicity and thermal properties of the nanofibres. The results from this study provide valuable insights into the understanding of the behaviour of silica nanoparticles and the method to fabricate superhydrophobic electrospun nanofibre membranes for MD application.

Keywords: Electrospinning, polyacrylonitrile, superhydrophobic, silica nanoparticles, membrane distillation

1. INTRODUCTION

High salinity water including wastewater produced from a variety of sources like desalination plants, oil and gas fields, mining, and industries, has had a detrimental effect and threat to the global environment, social welfare, and human health [1–3]. Over the years, various modern technologies for treating high salinity wastewater have been developed, including reverse osmosis, nanofiltration, ultrafiltration and microfiltration, etc. [4,5]. However, these desalination technologies typically consume a lot of energy due to the high operating temperatures and involving several complicated procedures. Membrane distillation (MD) which is a membrane-based thermal desalination process, has emerged as the most promising solution for treating high salinity wastewater [6]. Besides, MD is capable of producing a large amount of freshwater with a high rate of water recovery from saline feedwater by utilising low-grade energy generated from waste heat [7–9]. The high salt rejection efficiency of up to 99.99% and simple operating procedures also make MD attractive and competitive in desalination applications [10].

*nurfaizey@utem.edu.my

In an MD system, hydrophobic membranes were used as physical barriers for vapour transmission between the hot-feed side and cold-permeate side, filtering all non-volatiles solutes from feed water [11]. Nevertheless, a significant challenge arise when using MD to treat high-salinity wastewater caused by pore wetting, which degrades the performance of hydrophobic membranes and reduces vapour flux [12]. On the other hand, particulate matter in the feed water precipitates and accumulates on the membrane surface or within the membrane pores, causing a phenomenon known as membrane fouling [13]. Furthermore, the presence of salt crystals in the membrane pores would block the path of vapour transfer between the feed side and permeate side, causing the membrane prone to damage caused by hydraulic pressure. When the operating pressure is beyond the liquid entry pressure (LEP), the membranes would rupture, and the feed solution leaks through the membrane pores and contaminate the permeate side [14,15]. Apart from that, low surface-tension amphiphilic contaminants that are found in the feed water can also cause pore wetting by lowering the surface tension of the feed solution, which makes it easier for surfactants to be saturated in the surface of membrane pores [16,17]. Additionally, the existence of surfactants on the membrane surface would also change the behaviour of the hydrophobic membrane into the hydrophilic membrane [18].

In order to overcome membrane fouling and a continuously decreasing vapour flux during the desalination process, it is necessary to modify the properties of MD membranes using proper chemical and physical treatments. In particular, it has been proved that nanofibrous membranes fabricated by the electrospinning technique can effectively mitigate the membrane fouling and pore wetting due to their high porosity, narrow pore size distribution, and low tortuosity [19–22]. Electrospinning is defined as a simple and versatile process that draws fibres from a liquid polymer solution using strong electrostatic charges to form microporous membranes with interconnected structures through layer-by-layer of fibres [23–25]. The nanofibrous membrane would lower the mass transfer resistance inside the feed channel to produce higher vapour flux while maintaining its quality [26,27]. However, the nanofibrous membrane typically has weak interactions compared to the conventional microfiltration membranes [28]. This is because the asymmetrical hydraulic perturbation on both sides of the membrane causes a large pore deformation, allowing salt crystals to cross the hydrophobic membrane pores [29].

In many research scenarios, membrane modification is the best option to enhance the wetting properties and durability of the nanofibrous membrane [30,31]. Variety methods are currently used for the modification of MD membranes, such as interfacial polymerisation, graft polymerisation and dip coating [32]. The purpose of the modification process is to obtain the desired membrane characteristics, which may mitigate the challenges associated with MD process. For instance, the addition of nanoparticles compounds such as silver (Ag), silica (SiO_2) and titania (TiO_2) onto the MD membranes would roughen the membrane surface [32,33]. Besides, fluorinated reagents are commonly used as a post-treatment for the nanoparticles-modified membrane to improve the wettability of the membrane by lowering the surface energy [31,34]. It facilitates the formation of a superhydrophobic coating by enriching the surface with CF_3 groups and a surface water contact angle (WCA) of more than 150°. To date, a variety of superhydrophobic fibrous membranes have been used in the MD process, such as polytetrafluoroethylene (PTFE), polyurethane (PU), polypropylene (PP) and polyvinyl fluoride (PVDF) [35–37]. However, these fibrous membranes have a lot of limitations, and their flux remains unsatisfactory for practical applications [38]. Hence, developing strategies to optimise the MD membranes is crucial for achieving higher vapour flux and better antifouling performance.

In this study, a novel superhydrophobic nanofibrous membrane was developed by combining the privileges of electrospun nanofibers with surface modifications to produce a highly porous membrane structure with excellent wetting properties. Polyacrylonitrile (PAN) polymer was used as a precursor material due to excellent thermal stability, solvent resistance and possessed high mechanical strength [39–41]. The superhydrophobic membrane was fabricated by electrospinning of PAN polymer followed by the addition of SiO_2 nanoparticles via dip-coating

technique and fluorination surface treatment. An initial experiment was carried out to investigate the aggregation of nanoparticles on the nanofibre surface, which could result in reduced membrane pore size. The fabricated membranes were then characterised in terms of morphological, water contact angle and thermal properties. This study was carried out as part of the laboratory's ongoing effort to develop a functional superhydrophobic nanofibrous membrane for future implementation in MD process.

2. METHODOLOGY

Polyacrylonitrile (PAN) with a molecular weight of 150,000 g/mol and N, N-Dimethylformamide (DMF, ≥99.8%) from Sigma-Aldrich (Selangor, Malaysia) were used to produce PAN electrospun fibres. The PAN/DMF solution was prepared by dissolving PAN powder into DMF solution with a final concentration of 10 wt.%. The PAN/DMF solution was stirred at room temperature for approximately 4 – 6 hours until homogeneous using a magnetic stirrer model C-MAG HS7 (Ika Works, Malaysia). The PAN/DMF solution was placed in a 12 ml plastic syringe and attached to a syringe pump model NLS20 (Nanolab Instruments, Malaysia). Electrospinning model ES1a (Electrospinz Ltd., New Zealand) was used to produce PAN nanofibres membrane. The electrospinning apparatus consists of four main components, i.e., a high voltage power supply, a needle tip with a small orifice (also known as spinneret), a polymer solution supply, and a grounded collector electrode (Figure 1). The electrospinning process was conducted at a temperature of 24°C and relative humidity of 64%. The as-spun fibres were collected using an aluminium foil wrap around the surface of a rotating drum collector with a rotation speed of 120 revolutions per minute. The rotating drum collector was positioned 15 cm away from the spinneret, whilst the applied voltage was maintained at 15 kV, and the polymer feed rate was controlled with a syringe pump at 1.1 ml/h. The electrospinning processing parameters for the preparation of PAN electrospun fibres are tabulated in Table 1. These electrospinning process parameters were selected based on the best results obtained in a previous study [42]. The obtained PAN electrospun fibres were dried for 24 hours at room temperature. The samples were carefully cut to approximately 10 × 10 mm in length with an average mass of 0.30 mg and then peeled from the aluminium foil.

Table 1 Electrospinning Parameters for the Preparation of PAN Electrospun Fibres

Electrospinning Parameters	
Solution concentration	10 wt.%
Applied voltage	15 kV
Polymer feed rate	1.1 ml/h
Electrospinning distance	15 cm
Working temperature	24°C
Humidity	64%
Rotation speed of drum collector	120 rpm

The PAN electrospun fibres underwent a surface modification process with a SiO_2 nanoparticle coating followed by a fluorinated silane treatment. Tetraethyl orthosilicate (TEOS, ≥99%) and 1H,1H,2H,2H-Perfluorooctyltriethoxysilane (FOTS, 98%) obtained from Sigma-Aldrich (Selangor, Malaysia) were used for the preparation of SiO_2 nanoparticles solution and fluorinated silane treatment. Meanwhile, ammonium hydroxide 25% concentration supplied from Merck (Selangor, Malaysia) and ethanol (95%) obtained from Polyscientific (Melaka, Malaysia) were used as a solvent for coating agent solution. The SiO_2 nanoparticles were prepared by mixing TEOS/ethanol solution (5 ml of TEOS in 25 ml of ethanol) with the ammonium hydroxide /ethanol solution (6 ml of ammonium hydroxide in 25 ml of ethanol) for 10 min at room temperature using a magnetic

stirrer. The mixture was stirred until it turned into a milky solution. Then, the PAN electrospun fibres were immediately dip-coated in SiO_2 nanoparticles solution at different hydrolysis time (10, 20, 30, 40, 50 and 60 min). The coated PAN electrospun fibres membranes were dried overnight at room temperature. The fluorination surface treatment was conducted by immersing the coated fibres into 5% v/v of FOTS/ethanol solution for 10 min and dried at room temperature before finally being cured in an oven at 110°C for 60 min. This preparation method was done similarly according to Fang *et al.* [43]. The overall preparation of superhydrophobic PAN electrospun nanofibres membrane is illustrated in Figures 1 and 2.

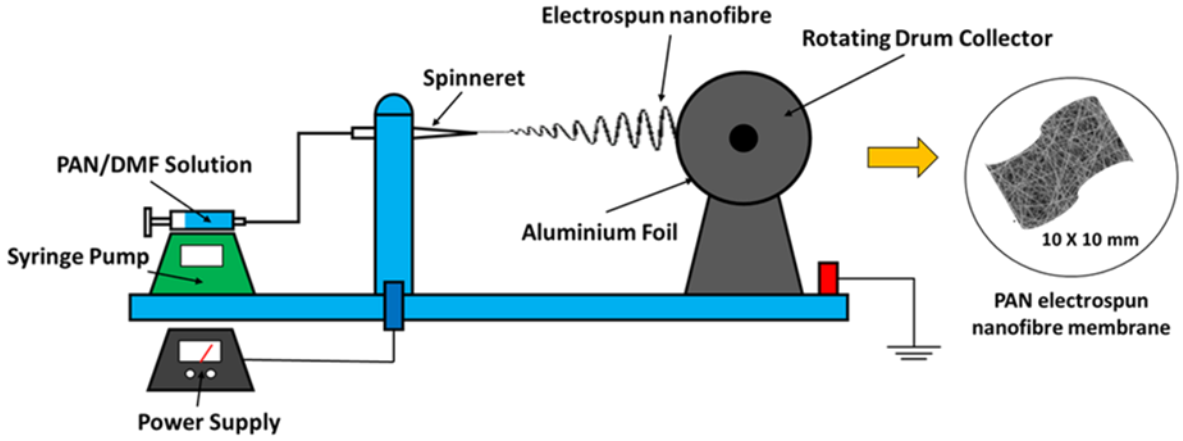

Figure 1. Schematic diagram of electrospinning process for the fabrication of PAN electrospun nanofibres membrane.

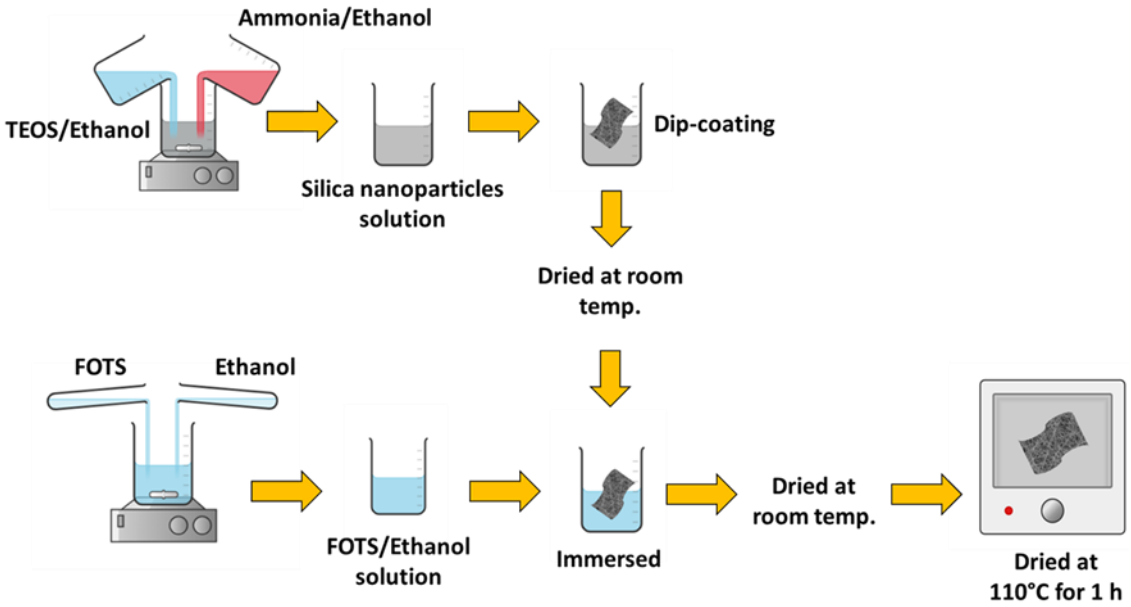

Figure 2. Schematic diagram of the preparation of SiO_2 nanoparticles solution and FOTS surface treatment for preparing superhydrophobic electrospun nanofibre membrane.

The morphology of coated PAN electrospun nanofibres membranes was examined using SEM model JSM-6010 PLUS/LV (Jeol Ltd., Japan). The obtained image was analysed using ImageJ version 1.50 software (National Institutes of Health, USA) to estimate the size of SiO_2 nanoparticles, fibre diameter and pore size. At least 100 measurements were taken randomly from each SEM micrograph. The porosity of coated PAN electrospun nanofibre membranes was estimated using the conventional porosity measurement method as shown in Equations 1 and 2

[43]. Since SiO_2 nanoparticle coating has a very minimal effect on the membrane thickness, thus the thickness of the membrane can be considered constant with an average thickness of 18.7 μm. Material density of PAN polymer of 1.184 g/cm^3 was used.

$$\text{Porosity } (\%) = 1 - \frac{\text{Density}_{\text{apparent}}(\text{g cm}^{-3})}{\text{Density}_{\text{material}}(\text{g cm}^{-3})} \times 100\% \quad (1)$$

$$\text{Density}_{\text{apparent}}(\text{g cm}^{-3}) = \frac{\text{Mass (g)}}{\text{Thickness (cm)} \times \text{Surface area (cm}^2\text{)}} \quad (2)$$

The hydrophobicity of coated and uncoated PAN electrospun nanofibre membranes was determined by capturing the image of the water droplet on the membrane surface using a dedicated contact angle instrument (A-CAM). A distilled water droplet (5 μl) was dripped at the centre of the membranes. The WCA of membranes was then measured using ImageJ version 1.50 software in accordance with the standard D5725-97 (ASTM, 2003). For every determination, the contact angle was measured five times to obtain accurate and precise results. The measurement method followed a similar approach that was used by Jasmee *et al*. [44].

To ensure the SiO_2 nanoparticles and FOTS were successfully embedded in the nanofibre membrane, the FTIR model Nicolet iS10 (Thermo Scientific, Malaysia) was recorded in ATR mode. Infrared spectra were recorded in the wavenumber range of 500–4000 cm^{-1}. The as-obtained result was compared to the uncoated PAN electrospun nanofibre. A DSC model DSC822e (Mettler Toledo, Malaysia) was used to measure the thermal properties of coated and uncoated PAN electrospun nanofibre membranes. The heating rate and nitrogen flow were set at 20°C/min and 50 ml/min, respectively. The fibres were then sealed in aluminium crucibles (40 μl), and the measurements were conducted in the temperature range of 25°C to 350°C.

3. RESULTS AND DISCUSSION

3.1 Surface Morphologies of PAN Electrospun Nanofibres

The average fibre diameter of PAN nanofibres membranes observed from SEM micrographs was 554 ± 54 nm. The SEM images in Figure 3 (a) to (f) showed that the concentration of SiO_2 nanoparticle compounds in the nanofibre membrane increased as the hydrolysis time increased. This was because the SiO_2 nanoparticle concentration kept increasing until TEOS was consumed completely [45]. The results showed that hydrolysis time has a significant impact on the concentration and size of silica nanoparticles. Hence, the membrane coating process must be performed immediately after the synthesis of the coating solution in order to observe the behaviour of SiO_2 nanoparticles accurately.

During the mixing of ammonium hydroxide in the TEOS/ethanol solution, the TEOS started hydrolysing and forming sphere-like nanoparticles. The addition of ammonium hydroxide as a catalyst agent will trigger the nucleation growth of the particles and continuously reacted, resulting in the particles aggregating and eventually producing larger particles [45]. As evidenced, the average size of SiO_2 nanoparticles measured after 10 minutes of hydrolysis was 343.60 nm, and the size continued to increase to around 577.80 nm after one hour of reaction, as shown in Table 2. In addition, the increase in particle size was observed to be substantially faster in the first half-hour. After 50 minutes of hydrolysis, the average SiO_2 nanoparticle size increased by only 3.10 nm from 574.70 to 577.80 nm, and the particle size kept constant afterwards.

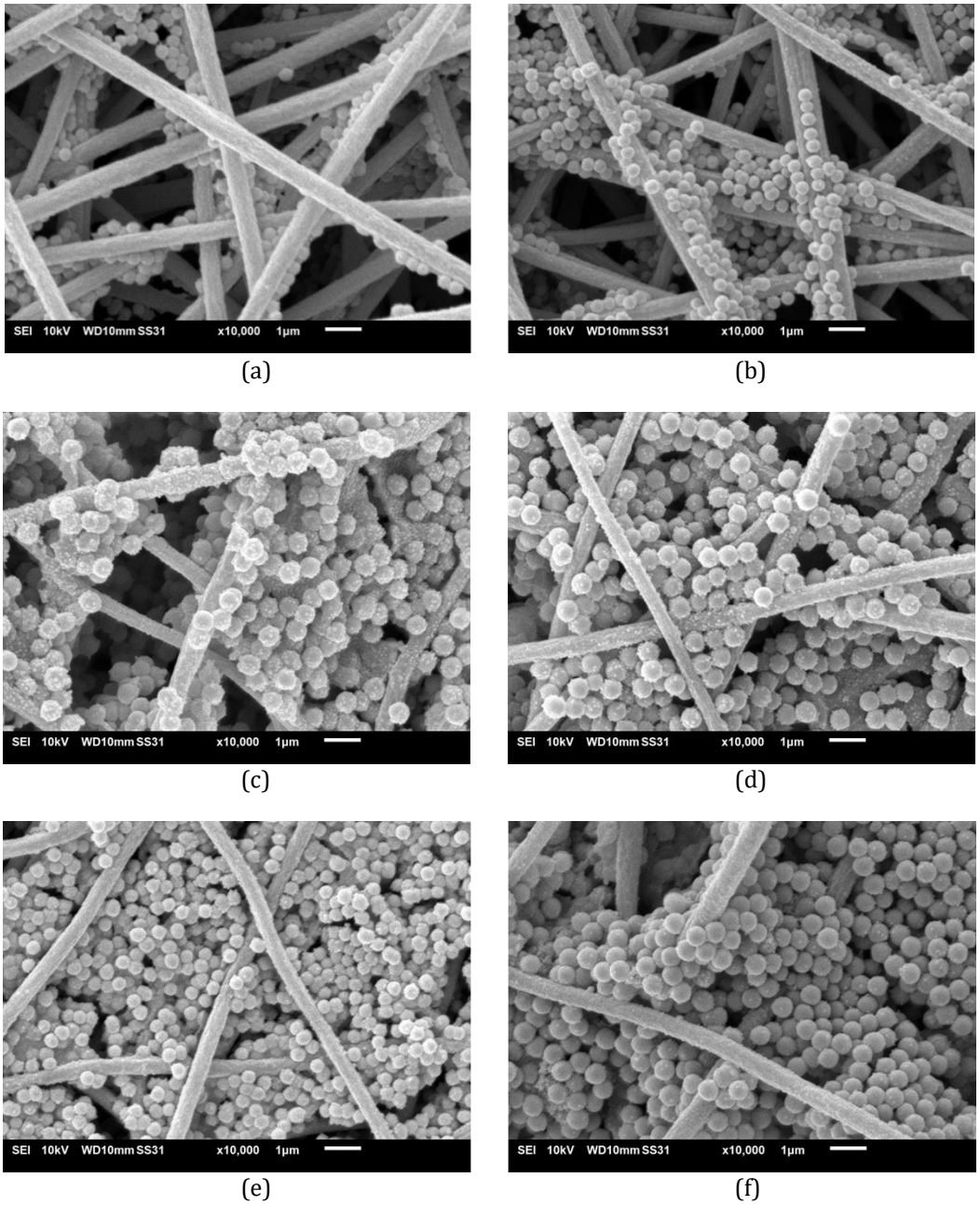

Figure 3. The SEM images of PAN electrospun nanofibres coated by SiO_2 nanoparticle solutions under a different duration of hydrolysis time (a) 10 min, (b) 20 min, (c) 30 min, (d) 40 min, (e) 50 min and (f) 60 min.

The intention of adding SiO_2 nanoparticles into PAN nanofibres membranes was to reduce membrane pore size, which would lessen the membrane fouling during the MD process. Based on Figure 3 (a) to (d), SiO_2 nanoparticles started agglomerating rapidly and filled the gaps between fibres. However, the longer the hydrolysis time, the higher the nanoparticle compounds in nanofibre membranes (Figure 3 (e) and (f)), which would block the vapour transfer during the separation process. Meanwhile, it was also discovered that the membrane pore size decreased from 994.56 nm to 275.20 nm as the hydrolysis time increased (Table 2). The selection of membrane pore size was crucial in determining the MD performance. This was because the larger pore size would easily allow saline water to pass through the membrane pore. On the contrary, a smaller pore size would slower the vapour transmission, resulting in low vapour flux [11].

Furthermore, the data in Table 2 shows that the porosity of coated PAN nanofibre membranes was similar throughout the hydrolysis time. This was probably due to the nanoparticles mainly staying only on the surface of the nanofibre membrane. Thus, it would not affect the internal porous structure. In general, the average porosity of coated PAN nanofibre observed was approximately 86.25%, which was concurrent with the previous study [43,46].

Based on Figure 4(a), fibres with glue-like and sticky structures were observed after the surface fluorination treatment. The presence of a sticky structure would hold the SiO_2 nanoparticles tidily and improve the interaction between nanoparticles and fibres. As shown in Figure 4 (b), SiO_2 nanoparticles adhere to the surface created by the FOTS treatment. On the other hand, the results suggest that the SiO_2 nanoparticles would remain on the membrane surface even after the MD separation process, resulting in increasing membrane lifespan.

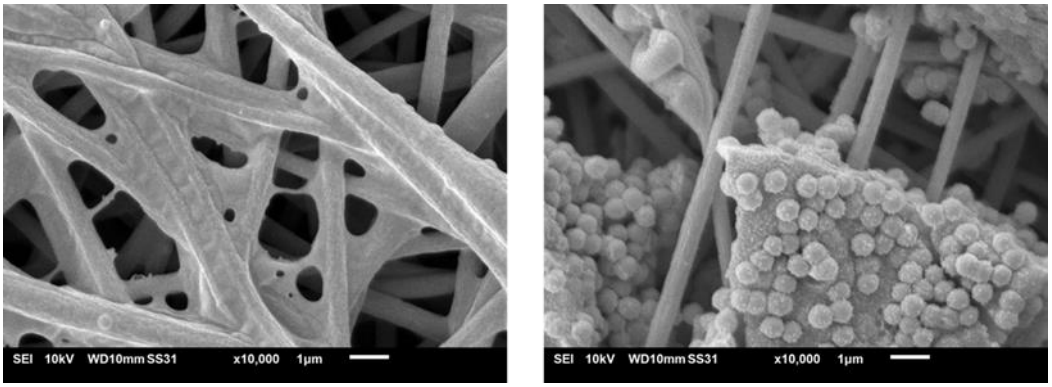

(a) (b)

Figure 4. The SEM images of PAN electrospun nanofibres coated by (a) FOTS and (b) SiO_2/FOTS.

Table 2 Effects of Hydrolysis Time on Silica Particle Size, Membrane Porosity and Pore Size

Hydrolysis time (min)	Nanoparticle size (nm)	Pore size (nm)	Porosity (%)
0 (uncoated)	-	994.56	86.56
10	343.60	844.25	84.83
20	369.80	608.33	86.04
30	391.10	486.80	87.45
40	547.40	339.63	87.23
50	574.70	333.73	86.44
60	577.80	275.20	85.52

3.2 Hydrophobicity of PAN Electrospun Nanofibres

The surface wetting behaviour of PAN nanofibre membranes was determined by measuring the water contact angle (WCA) via ImageJ software. According to Figure 5(a), the average WCA of pure PAN nanofibre membrane was 121.23°. This value shows that pure PAN electrospun fibres possessed a hydrophobic behaviour. Additionally, it was observed that when distilled water was dripped vertically onto PAN nanofibre membranes, the water droplet retained its shape for a brief period. However, the water droplet could only maintain its shape for about 6 to 8 seconds before rupturing. This was due to the fact that the forces associated with interactions between the nanofibre surface and water droplet were eventually greater than the bulk water, resulting in a decrease in surface tensions [47].

Furthermore, membrane modification through SiO_2 nanoparticles coating and FOTS surface treatment significantly increased the surface hydrophobicity of PAN nanofibres. As shown in Figure 5(b), the average WCA for PAN nanofibre coated with SiO_2 nanoparticles was 131.64°, slightly higher than pure PAN nanofibre membrane. This was because SiO_2 nanoparticles fill the gap between the fibres and thus increase the surface roughness [33]. Apparently, if the nanofibre membranes were just coated with SiO_2 nanoparticles, without any fluorination surface treatment, the WCA was always less than 150°.

Figure 5(c) shows that the WCA of the PAN/SiO_2/FOTS nanofibre membrane was 151.02°, indicating that the modified PAN membranes have excellent water repellence properties. The increase in surface hydrophobicity was due to the presence of CF_3 from FOTS substances, which reduced the surface free energy [48]. Apart from that, it was also observed that the water droplet did not adhere to the membrane surface even when the membranes were placed vertically, suggesting a low water affinity. Notably, the low adhesion properties of treated PAN nanofibre membranes would prevent blockage within the membrane pores, which is advantageous for the water separation process [49]. Hence, it was concluded that by using this approach, the WCA of PAN nanofibre membranes increased from 121.23° to 151.02°.

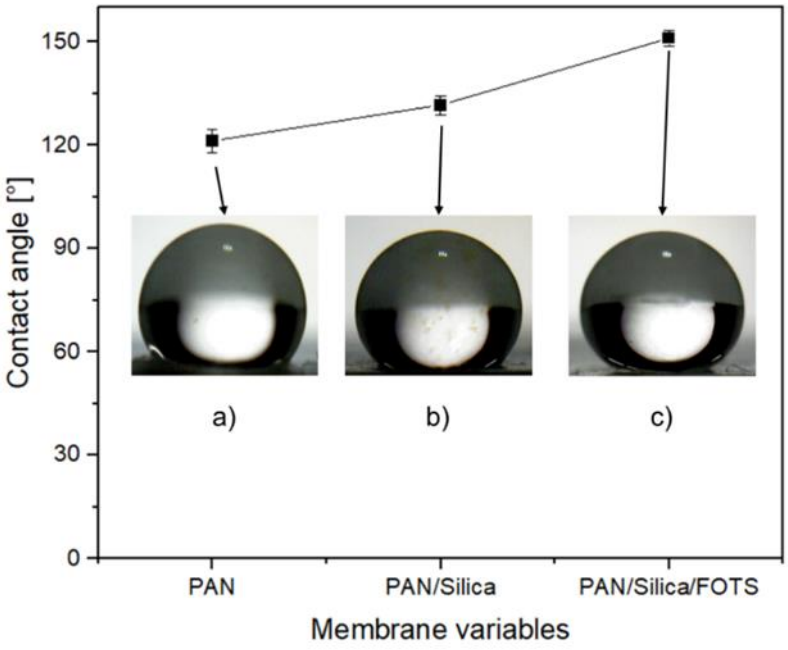

Figure 5. Water contact angle (WCA) of a) pure PAN, b) PAN/SiO_2 and c) PAN/SiO_2/FOTS nanofibre membrane.

3.3 Chemical Structure Characterisation

The chemical structure of uncoated and coated PAN nanofibre membranes was identified by FTIR spectra, as shown in Figure 6. According to the spectrum, the pure PAN nanofibre membrane showed distinctive peaks at 2939 cm^{-1} and 1452 cm^{-1}. These vibration peaks are typically attributed to the asymmetrical and symmetrical bending of C-H, respectively [48,50,51]. Meanwhile, the nitrile (C≡N) stretching peak can be recognised at 2242 cm^{-1}. Besides, the peak at 3679 cm^{-1} represents aliphatic O-H, which was formed from dimethylformamide acid that remained after the electrospinning process [52]. Apart from that, when the SiO_2 nanoparticles were added into the PAN nanofibre membrane, new peaks located at 1073 cm^{-1}, 953 cm^{-1} and 794 cm^{-1} appeared, which corresponds to Si-O-Si symmetric stretching vibration and bending vibration [43,53]. Furthermore, it was also observed that after FOTS surface treatment, it introduced a new peak at 1131 cm^{-1}, which resulted from the C-F in 1H,1H,2H,2H-perfluorooctyl

groups [54]. The result indicated that SiO_2 nanoparticles and FOTS were successfully embedded into PAN nanofibre membranes.

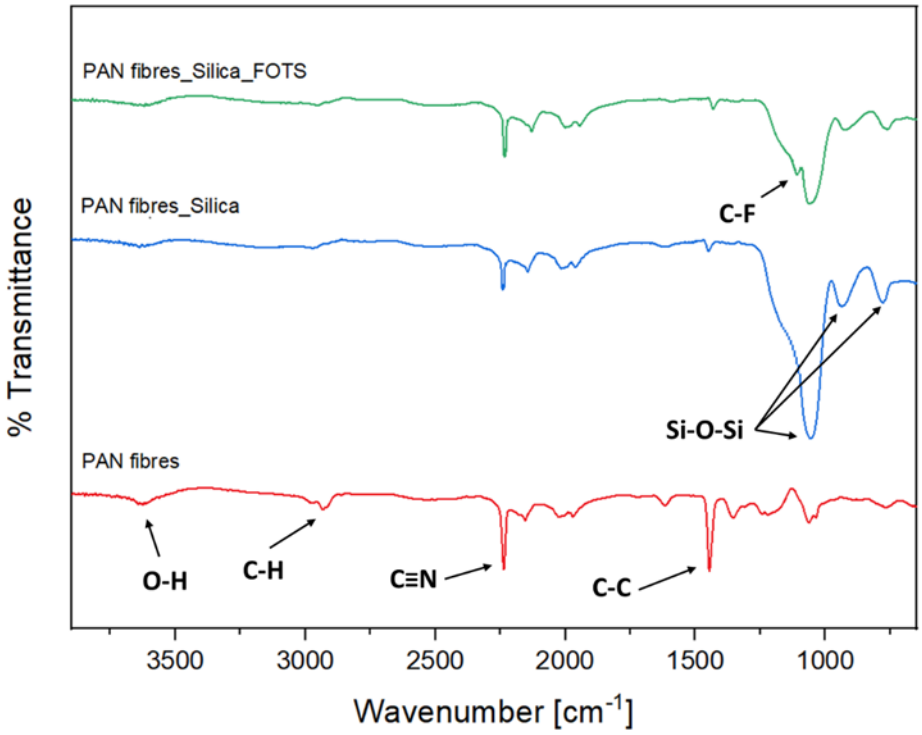

Figure 6. FTIR spectra of pure PAN, PAN/SiO_2 and PAN/SiO_2/FOTS nanofibre membrane.

3.4 Thermal Property of PAN Electrospun Nanofibres

DSC analysis was carried out to measure the glass transition temperature (T_g) of uncoated and coated PAN nanofibre membranes. As shown in Figure 7, the T_g of pure PAN nanofiber membranes observed was 101 °C. However, after the membrane was coated with SiO_2 nanoparticles, the T_g value increased to a higher temperature (148 °C). This was most likely caused by the conversion of crystalline domains to an amorphous structure due to the formation of crosslinked structures between PAN chains and silanol groups via the formation of Si-O-Si bonds [4]. Hence, the molecular structure of PAN became more ordered, which constrained the movements of molecular chains, resulting in an increase in T_g. Furthermore, when the PAN/SiO_2 membrane was coated with FOTS, the T_g value decreased slightly to 137 °C. A similar finding was reported by Mustafa Çakır [55], who stated that the presence of fluorine content would cause a decrease in T_g values.

According to Figure 7, the observed exothermic peak of PAN nanofibre membranes was 321.7 °C, and the peak position shifted to a higher temperature of around 342.3 °C for PAN/SiO_2 and 326.6 °C for PAN/ SiO_2/FOTS membrane. The results illustrated that the PAN nanofibre membrane tend to degrade around 321.7 °C and the addition of SiO_2 nanoparticles and FOTS treatment suggests that it requires more energy to break down the cyclic structure. Moreover, the intensity of the exothermic peak was observed to decrease and begin to broaden, which could be attributed to the decreased mobility of the crystalline domains in PAN and the increased polymer chain stiffness and amorphous nature caused by the cyclisation and crosslinking reaction [47,56]. Therefore, the result proved that the addition of SiO_2 nanoparticles and FOTS treatment significantly influence the thermal properties and durability of PAN nanofibre membranes.

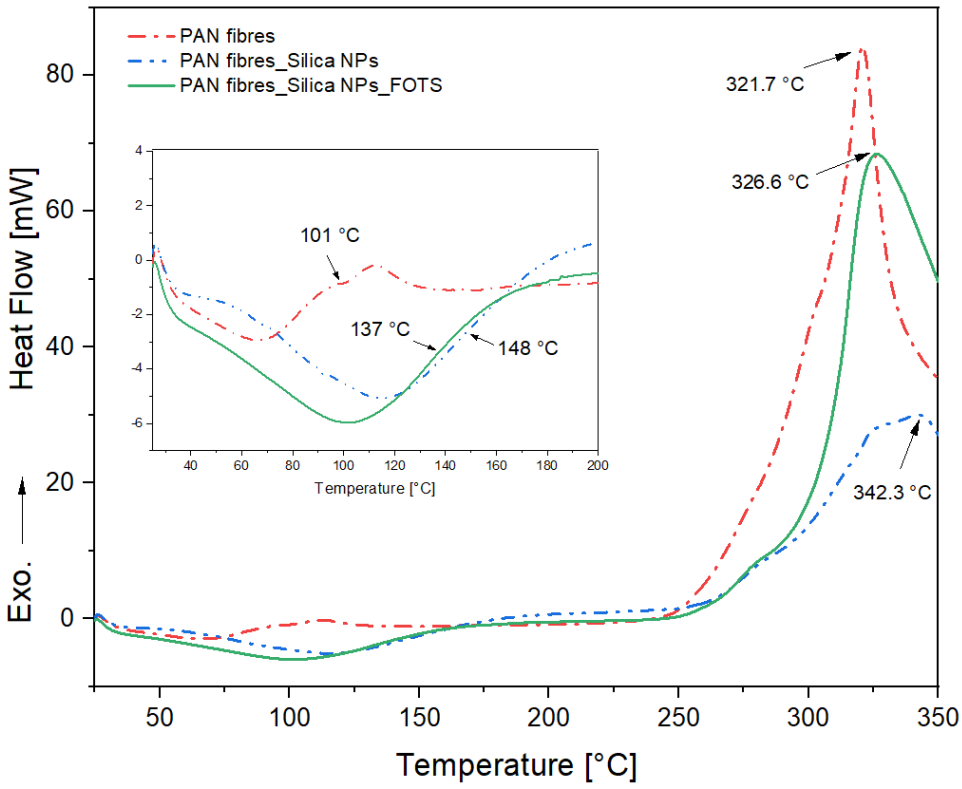

Figure 7. DSC curves of pure PAN, PAN/SiO_2 and PAN/SiO_2/FOTS nanofibre membrane.

Recently, various research efforts have been made to develop highly effective MD membranes by modifying the surface morphology and configurations. In MD technology, membranes with a high porosity structure and superhydrophobic properties are preferable due to their ability to mitigate the membrane wetting and increase the vapour flux [57]. In this study, PAN electrospun nanofibres were used as a precursor material, followed by SiO_2 nanoparticle surface coating and fluorination surface treatment to create superhydrophobic nanofibre membranes. The result of this study suggests that PAN electrospun nanofibre membranes have the potentials to be used as coating materials for the development of MD membranes due to their small pore size, high hydrophobicity, and excellent thermal stability.

4. CONCLUSION

In summary, superhydrophobic nanofibre membranes were successfully fabricated by coating polyacrylonitrile (PAN) nanofibre membranes with SiO_2 nanoparticles and FOTS surface treatment. The SiO_2 nanoparticles were prepared by hydrolysis of TEOS and ethanol and followed by the addition of ammonium hydroxide. According to characterisation results, hydrolysis time had a significant effect on particle loading on nanofibre membranes. As the hydrolysis time increased from 10 min to 60 min, the SiO_2 nanoparticles started to grow from 343.60 nm to 577.80 nm and agglomerate rapidly to occupy the space between the fibres. Thus, the membrane pore size reduced from 994.56 nm to 275.20 nm. In terms of membrane porosity, the porosity of PAN nanofibre membranes remains constant, with an average porosity of 86.25%, whether uncoated or coated. After the membrane modification, it was found that the water contact angle (WCA) of PAN nanofibre increased from 121.23° to 151.02°. The results indicate that the PAN/SiO_2/FOTS nanofibre membrane exhibit superhydrophobicity due to its extremely low surface free energy and high surface roughness. The thermal property showed that the coated PAN/SiO_2/FOTS nanofibre membrane begins to degrade when the temperature is beyond 342.3 °C, indicating that it has a high thermal resistance. This study demonstrates that combining the

topology and surface chemistry of electrospun nanofibres results in superhydrophobic nanofibre membranes that could potentially be used in membrane distillation technology.

ACKNOWLEDGEMENTS

The authors would like to thank the Ministry of Higher Education Malaysia and Universiti Teknikal Malaysia Melaka through the funding of Collaborative Research Grant PJP/2019/FKM-CARE/CRG/S01706. Special thanks to the members of Advanced Materials Characterization Laboratory (UTeM), Academia-Industry Collaboration Laboratory, the members of the Faculty of Mechanical Engineering, UTeM, and Advanced Membrane Technology Research Centre (AMTEC), UTM.

REFERENCES

[1] Zhu, Z., Wang, W., Zhang, Q., and Chen, X., J. Memb. Sci. vol **620** (2021) pp.1–9.
[2] Younssi, S. A., Breida, M., and Achiou, B., Desalin. Water Treat. (2018) pp.221–254.
[3] Sahu, P., J. Water Reuse Desalin. vol **11**, issue 1 (2021) pp.33–65.
[4] Chaudhri, S. G., Chaudhari, J. C., and Singh, P. S., J. Appl. Polym. Sci. vol **135**, issue 3 (2018) pp.1–13.
[5] Ruiz-García, A., Melián-Martel, N., and Nuez, I., Membranes (Basel). vol **7**, issue 4 (2017) pp.1–17.
[6] Pistocchi, A., Bleninger, T., Breyer, C., Caldera, U., Dorati, C., Ganora, D., Millán, M. M., Paton, C., Poullis, D., Herrero, F. S., Sapiano, M., Semiat, R., Sommariva, C., Yuece, S., and Zaragoza, G., Water Res. vol **182** (2020) .
[7] An, A. K., Guo, J., Jeong, S., Lee, E. J., Tabatabai, S. A. A., and Leiknes, T. O., Water Res. (2016) .
[8] Li, S., Huang, J., Chen, Z., Chen, G., and Lai, Y., J. Mater. Chem. A vol **5**, issue 1 (2017) pp.31–55.
[9] Roy, S., Humoud, M. S., Intrchom, W., and Mitra, S., ACS Sustain. Chem. Eng. (2018) .
[10] Essalhi, M., Khayet, M., Tesfalidet, S., Alsultan, M., and Tavajohi, N., Chem. Eng. J. vol **426**, issue April (2021) p.131316.
[11] Thi Tra My, N., Thi Yen Nhi, V., and Xuan Thanh, B., J. Appl. Membr. Sci. Technol. vol **22**, issue 1 (2018) .
[12] Dong, S., Yun, Y., Wang, M., Li, C., Fu, H., Li, X., Yang, W., and Liu, G., J. Taiwan Inst. Chem. Eng. vol **117** (2020) pp.56–62.
[13] Zhu, Z., Zhong, L., Horseman, T., Liu, Z., Zeng, G., Li, Z., Lin, S., and Wang, W., J. Memb. Sci., issue June (2020) p.118768.
[14] Deshmukh, A., Boo, C., Karanikola, V., Lin, S., Straub, A. P., Tong, T., Warsinger, D. M., and Elimelech, M., Energy Environ. Sci. (2018) .
[15] Warsinger, D. M., Servi, A., Connors, G. B., Mavukkandy, M. O., Arafat, H. A., Gleason, K. K., and Lienhard, J. H., Environ. Sci. Water Res. Technol. vol **3**, issue 5 (2017) pp.930–939.
[16] Wang, Z., Chen, Y., Zhang, F., and Lin, S., Desalination vol **450**, issue October 2018 (2019) pp.46–53.
[17] Rezaei, M., Warsinger, D. M., Lienhard V, J. H., Duke, M. C., Matsuura, T., and Samhaber, W. M., Water Res. (2018) .
[18] Su, Q., Zhang, J., and Zhang, L. Z., Desalination vol **476**, issue December 2019 (2020) p.114246.
[19] Nurfaizey, A. H., Long, F. C., Daud, M. A. M., Muhammad, N., Mansor, M. R., and Tucker, N., J. Mech. Eng. Sci. vol **13**, issue 1 (2019) pp.4679–4692.
[20] Zhu, Z., Liu, Z., Zhong, L., Song, C., Shi, W., Cui, F., and Wang, W., J. Memb. Sci. (2018) .
[21] Sheng, J., Xu, Y., Yu, J., and Ding, B., ACS Appl. Mater. Interfaces vol **9**, issue 17 (2017) pp.15139–15147.

[22] Tang, M., Hou, D., Ding, C., Wang, K., Wang, D., and Wang, J., Sci. Total Environ. vol **696** (2019) p.133883.
[23] Nurfaizey, A. H., Akop, M. Z., Salim, M. A., Mohd Rosli, M. A., and Masripan, N. A., World J. Eng. vol **17**, issue 1 (2020) pp.52–59.
[24] Nurfaizey, A., Roslan, N., Hafiz, M., Rosli, M., Saad, A., and Tucker, N., J. Adv. Manuf. Technol. vol **14**, issue 2(1) (2020) pp.91–100.
[25] Nurfaizey, A., Long, F., Daud, M., Masripan, N., and Tucker, N., J. Adv. Manuf. Technol. vol **14**, issue 2(1) (2020) pp.1–11.
[26] Huang, Y. X., Wang, Z., Jin, J., and Lin, S., Environ. Sci. Technol. (2017) .
[27] Liao, Y., Zheng, G., Huang, J. J., Tian, M., and Wang, R., J. Memb. Sci. (2020) .
[28] Su, C., Lu, C., Horseman, T., Cao, H., Duan, F., Li, L., Li, M., and Li, Y., J. Memb. Sci. vol **595**, issue September 2019 (2020) p.117548.
[29] Su, C., Lu, C., Cao, H., Tang, K., Chang, J., Duan, F., Ma, X., and Li, Y., J. Memb. Sci. vol **562**, issue January (2018) pp.38–46.
[30] Seo, D. H., Pineda, S., Woo, Y. C., Xie, M., Murdock, A. T., Ang, E. Y. M., Jiao, Y., Park, M. J., Lim, S. Il, Lawn, M., Borghi, F. F., Han, Z. J., Gray, S., Millar, G., Du, A., Shon, H. K., Ng, T. Y., and Ostrikov, K., Nat. Commun. vol **9**, issue 1 (2018) pp.1–12.
[31] Liu, L., Shen, F., Chen, X., Luo, J., Su, Y., Wu, H., and Wan, Y., J. Memb. Sci. vol **499** (2016) pp.544–554.
[32] Nthunya, L. N., Gutierrez, L., Derese, S., Nxumalo, E. N., Verliefde, A. R., Mamba, B. B., and Mhlanga, S. D., J. Chem. Technol. Biotechnol. vol **94**, issue 9 (2019) pp.2757–2771.
[33] Rostami, A., Pirsaheb, M., Moradi, G., and Derakhshan, A. A., Polym. Adv. Technol. vol **31**, issue 5 (2020) pp.941–956.
[34] Ebrahimi, F., Orooji, Y., and Razmjou, A., Polymers (Basel). (2020) .
[35] Kusuma, N. C., Purwanto, M., Sudrajat, M. A., Jaafar, J., Othman, M. H. D., Aziz, M. H. A., Raharjo, Y., and Qtaishat, M. R., J. Environ. Chem. Eng. vol **9**, issue 4 (2021) p.105582.
[36] Damtie, M. M., Kim, B., Woo, Y. C., and Choi, J. S., Chemosphere (2018) .
[37] Shao, Y., Han, M., Wang, Y., Li, G., Xiao, W., Li, X., Wu, X., Ruan, X., Yan, X., He, G., and Jiang, X., J. Memb. Sci. vol **579**, issue February (2019) pp.240–252.
[38] Horseman, T., Su, C., Christie, K. S. S., and Lin, S., Environ. Sci. Technol. Lett. vol **6**, issue 7 (2019) pp.423–429.
[39] Liang, W., Chenyang, Y., Bin, Z., Xiaona, W., Zijun, Y., Lixiang, Z., Hongwei, Z., and Nanwen, L., J. Memb. Sci. vol **569** (2019) pp.157–165.
[40] Ahmadi, Z., Ravandi, S. A. H., Haghighat, F., and Dabirian, F., Fibers Polym. vol **21**, issue 6 (2020) pp.1200–1211.
[41] Ryšánek, P., Benada, O., Tokarský, J., Syrový, M., Čapková, P., and Pavlík, J., Mater. Sci. Eng. C vol **105**, issue June (2019) .
[42] Arif, M. W. A., Nurfaizey, A. H., Mustafa, Z., Nadlene, R., Jaafar, J., and Tucker, N., Int. J. Nanoelectron. Mater. vol **14**, issue August (2021) pp.213–224.
[43] Fang, J., Wang, H., Wang, X., and Lin, T., J. Text. Inst. vol **103**, issue 9 (2012) pp.937–944.
[44] Jasmee, S., Omar, G., Masripan, N. A. B., Kamarolzaman, A. A., Ashikin, A. S., and Che Ani, F., Mater. Res. Express vol **5**, issue 9 (2018) .
[45] Norazmi, F. S., Chaudhary, K. T., Mazalan, E., Hader, Z., and Ali, J., Malaysian J. Fundam. Appl. Sci. vol **14** (2018) pp.482–484.
[46] Naseeb, N., Mohammed, A. A., Laoui, T., and Khan, Z., Materials (Basel). vol **12**, issue 2 (2019) pp.1–13.
[47] Alarifi, I. M., Alharbi, A., Khan, W. S., Swindle, A., and Asmatulu, R., Materials (Basel). vol **8**, issue 10 (2015) pp.7017–7031.
[48] Almasian, A., Chizari Fard, G., Mirjalili, M., and Parvinzadeh Gashti, M., J. Ind. Eng. Chem. vol **62** (2018) pp.146–155.
[49] Zhang, Z., Yang, Y., Li, C., and Liu, R., J. Memb. Sci. vol **582**, issue December 2018 (2019) pp.350–357.
[50] Lee, J., Yoon, J., Kim, J. H., Lee, T., and Byun, H., J. Appl. Polym. Sci. vol **135**, issue 7 (2018) pp.1–9.

[51] Sabantina, L., Rodríguez-Cano, M. Á., Klöcker, M., García-Mateos, F. J., Ternero-Hidalgo, J. J., Al Mamun, Beermann, F., Schwakenberg, M., Voigt, A. L., Rodríguez-Mirasol, J., Cordero, T., and Ehrmann, A., Polymers (Basel). vol **10**, issue 7 (2018).
[52] Munajat, N. A., Nurfaizey, A. H., Bahar, A. A. M., You, K. Y., Fadzullah, S. H. S. M., and Omar, G., Microw. Opt. Technol. Lett. vol **60**, issue 9 (2018) pp.2198–2204.
[53] Cai, Y., Li, J., Yi, L., Yan, X., and Li, J., Appl. Surf. Sci. vol **450** (2018) pp.102–111.
[54] Aleeva, Y., Ferrara, V., Bonasera, A., Martino, D. C., and Pignataro, B., Colloids Surfaces A Physicochem. Eng. Asp. vol **631**, issue June (2021) p.127633.
[55] Çakır, M., Coatings vol **7**, issue 3 (2017) p.37.
[56] Munajat, N. A., Nurfaizey, A. H., Husin, M. H. M., Siti Hajar, S. H. S., Omar, G., and Salim, M. A., J. Adv. Res. Fluid Mech. Therm. Sci. vol **49**, issue 2 (2018) pp.85–91.
[57] Muhamad, N. A. S., Mokhtar, N. M., Naim, R., Lau, W. J., and Ismail, A. F., Int. J. Eng. Technol. Sci. vol **6**, issue June (2019) pp.62–81.